



# CHORUS

This is the accepted manuscript made available via CHORUS. The article has been published as:

## Intermittent Molecular Hopping at the Solid-Liquid Interface

Michael J. Skaug, Joshua Mabry, and Daniel K. Schwartz

Phys. Rev. Lett. **110**, 256101 — Published 20 June 2013

DOI: [10.1103/PhysRevLett.110.256101](https://doi.org/10.1103/PhysRevLett.110.256101)

## Intermittent Molecular Hopping at the Solid-Liquid Interface

Michael J. Skaug, Joshua Mabry and Daniel K. Schwartz\*

Department of Chemical and Biological Engineering, University of Colorado Boulder,  
Boulder, CO 80309, USA

\*To whom communication should be addressed: [daniel.schwartz@colorado.edu](mailto:daniel.schwartz@colorado.edu)

### Abstract

The mobility of molecules on a solid surface plays a key role in diverse phenomena such as friction and self-assembly and in surface-based technologies like heterogeneous catalysis and molecular targeting. To understand and control these surface processes, a universally applicable model of surface transport at solid-liquid interfaces is needed. However, unlike diffusion at a solid-gas interface, little is known about the mechanisms of diffusion at a solid-liquid interface. Using single-molecule tracking at a solid-liquid interface, we found that a diverse set of molecules underwent intermittent random walks with non-Gaussian displacements. This contrasts with the normal random walk and Gaussian statistics that are commonly assumed for molecular surface diffusion. The molecules became temporarily immobilized for random waiting times between surface displacements produced by excursions through the bulk fluid. A common power-law distribution of waiting times indicated a spectrum of binding energies. We propose that intermittent hopping is universal to molecular surface diffusion at a solid-liquid interface.

In the context of interfacial transport, the solid-liquid and solid-gas interfaces are unique because the dynamics on either side of the interface are often radically different and adsorbate dynamics may depend on one or both of the bulk phases. At a solid-gas interface, adsorbate dynamics are dictated by the solid, which imposes a landscape of energy barriers. Scanning probe and field ion microscopy experiments have revealed activated hopping as the dominant mechanism controlling atomic and molecular transport at solid-gas interfaces [1, 2]. Less is known about adsorbate dynamics at the solid-liquid interface because, until recently, there were no experimental techniques that could reveal single-molecule trajectories. Recent single-molecule tracking experiments have exposed surface dynamics with multiple diffusive modes and desorption-mediated displacements [3, 4]. These findings do not fit the model for transport at the solid-gas interface, yet no equivalent model exists for transport at the solid-liquid interface, despite its importance.

Processes such as friction [5, 6] and self-assembly [7-9] and surface-based technologies like heterogeneous catalysis [10] and molecular targeting [11, 12] are influenced by the mobility of molecules on a solid surface. For example, intervals of surface diffusion can dramatically increase reaction rates [13, 14] over their bulk values. To understand and control these surface processes, a universal model of surface transport at solid-liquid interfaces is needed. To address this need, we used single-molecule tracking to track the motion of molecules at a model solid-liquid interface. We found that a diverse set of molecules, including a linear homopolymer, a globular protein and a small organic molecule, became temporarily immobilized for random waiting times between surface displacements produced by excursions through the bulk fluid. This contrasts with the 2-dimensional random walk and Gaussian statistics that are commonly assumed for molecular surface diffusion. We propose that intermittent hopping is universal to

molecular surface diffusion at a solid-liquid interface. This proposed model would modify our understanding of confined and surface-bound molecules [15, 16], and reveal new strategies for mimicking efficient biological targeting [17].

We used total internal reflection fluorescence microscopy (TIRFM) [18] to track the motion of individual molecules at a planar interface between water and polished fused silica, coated with a hydrophobic trimethylsilyl (TMS) monolayer. Surface preparation was previously described [19]. In each experiment, the water contained a low concentration (10 fM – 100 pM) of a particular fluorescent probe that randomly adsorbed, diffused on the surface and desorbed. We studied four probe molecules (Fig. 1): polyethylene glycol (PEG, Nanocs, USA), a 40,000 MW linear homopolymer end-labeled with fluorescein isothiocyanate; bovine serum albumin (BSA, Life Technologies, USA), a complex 66,500 MW protein labeled with ~5 AlexaFluor 555 dyes; Atto Rho6G (Atto6G, ATTO-TECH GmbH, Germany), a fluorescent rhodamine derivative; and BODIPY (Life Technologies, USA), a small hydrophobic fluorescent molecule. Between  $10^4$  and  $10^5$  trajectories were recorded for each molecule.

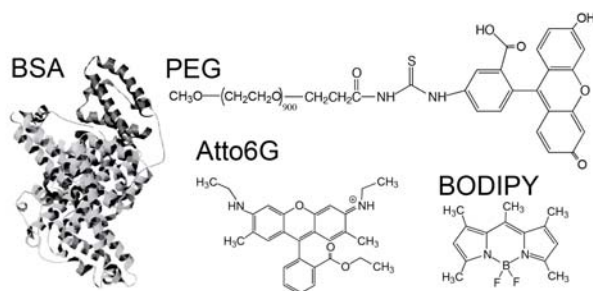


Fig. 1. Chemical structures of the four molecules studied.

The experimental exposure times were  $t_{\text{exp}} = 50\text{-}100$  ms. Due to high mobility in the aqueous bulk, the probe molecules were resolved only when they were adsorbed to the

surface. Image sequences were processed, and single-molecule tracking was performed as previously described [19]. Trajectories were constructed by connecting nearest neighbor objects in consecutive images given a maximum allowed displacement of  $R_{\max} = 5.8 \mu\text{m}$  for PEG, BSA and Atto6G and  $R_{\max} = 7.2 \mu\text{m}$  for BODIPY. The possibility of falsely connecting two molecules into a single trajectory is discussed in the supplementary material [25].

Fig. 2(b) shows a representative group of PEG trajectories. Some molecular trajectories appeared immobilized while others were highly mobile. Many trajectories switched between periods of immobilization and mobility. Despite their vast difference in size and complexity, all the molecules exhibited the same general intermittent behavior, although their overall mobility varied.

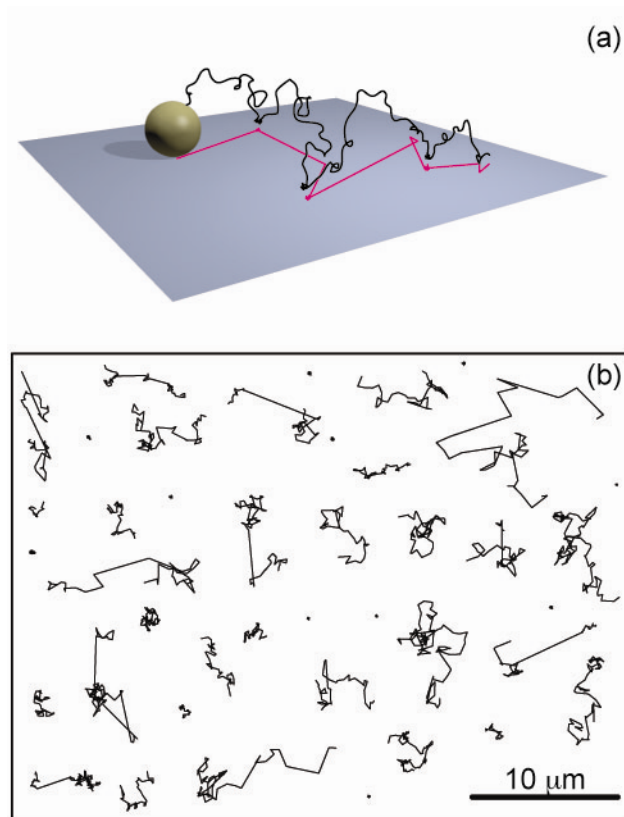


Fig. 2. (color online). (a) Schematic diagram of molecular surface diffusion that combines periods of immobilization with episodes of bulk diffusion above the surface. The black curve is the true 3D molecular trajectory and the magenta line is the effective 2D trajectory across the surface. (b) Example trajectories of PEG at the hydrophobic TMS-water interface. Each trajectory shown is greater than 4 s in length. A spectrum of intermittent behavior was observed, from completely mobile trajectories to trajectories that were immobile for their entire length.

Intermittent dynamics and periods of immobilization were reflected in the distributions of molecular displacements (Fig. 3), which were quantified in terms of the self-part of the van Hove correlation function [20],

$$G_s(\Delta x, \Delta t) = \frac{1}{N} \left\langle \sum_{i=1}^N \delta(x + x_i(t) - x_i(t + \Delta t)) \right\rangle, \quad (1)$$

where  $\langle \cdot \rangle$  indicates ensemble averaging. This distribution represents the probability that a molecule has moved a distance  $\Delta x$  along the x or y coordinate during time  $\Delta t$ . The distributions are not Gaussian, as one would assume for a simple diffusion process. Rather, they have a narrow Gaussian peak and extended tails, that are approximately Gaussian only in the case of BODIPY, the smallest molecule studied. The narrow, central peaks are associated with *apparent* displacements during periods of immobilization (or highly-constrained confinement), and do not broaden as a function of time (Fig. 3(b)). The width of the central peaks,  $\sigma \sim 0.065 \mu\text{m}$ , is consistent with imperfect localization of the molecules in each image and is a reasonable estimate of our experimental localization precision. The extended, non-Gaussian tails are the result of true displacements across the surface.

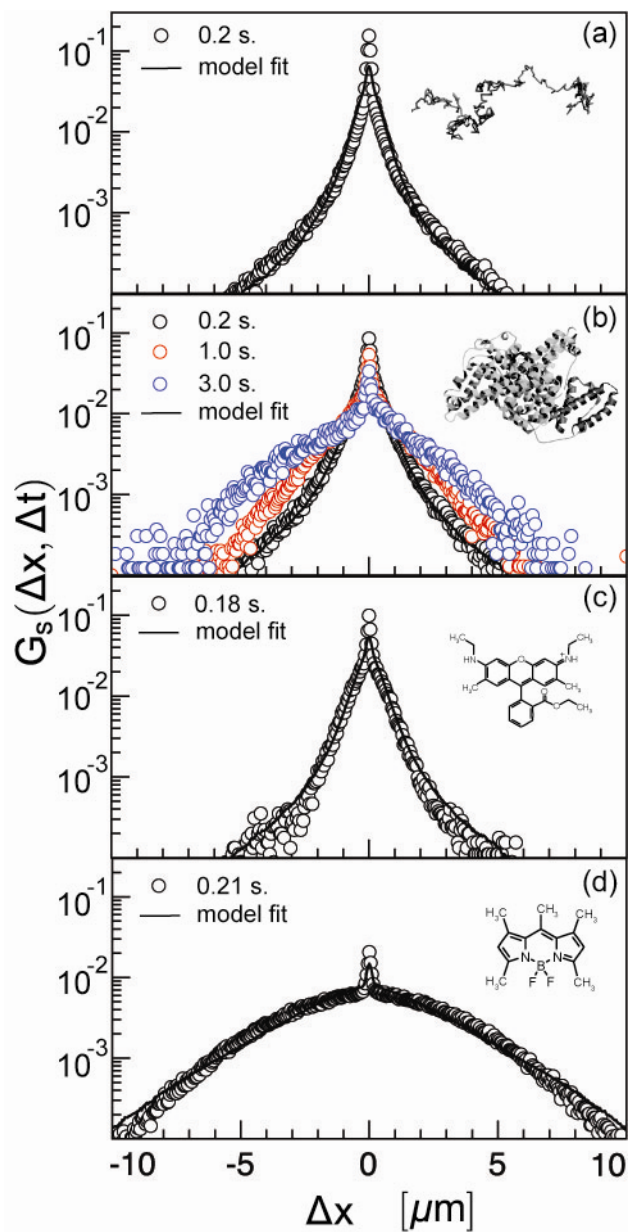


Fig. 3. (color online). Distributions of molecular surface displacements (Eq. (1)). Displacement distributions at the annotated  $\Delta t$  for (a) PEG, (b) BSA, (c) Atto6G, and (d) BODIPY. Symbols are experimental data measured using single-molecule tracking and the solid lines are simulated data using the model described in the text.

In Fig. 3, the tails of  $G_s$  exhibit decay that is slower than exponential and possibly power-law distributed, like that predicted for interfacial diffusion, when displacements occur via desorption, bulk diffusion and subsequent readsorption at the interface [3, 21]. We found that for some molecules, the tails became approximately Gaussian at longer times (Fig. 3(b)). After many individual displacements,  $G_s$  converges to a stable distribution, which for desorption-mediated steps is a Cauchy distribution [21] that would appear Gaussian at small displacements. This convergence was supported by our simulation results for BODIPY.

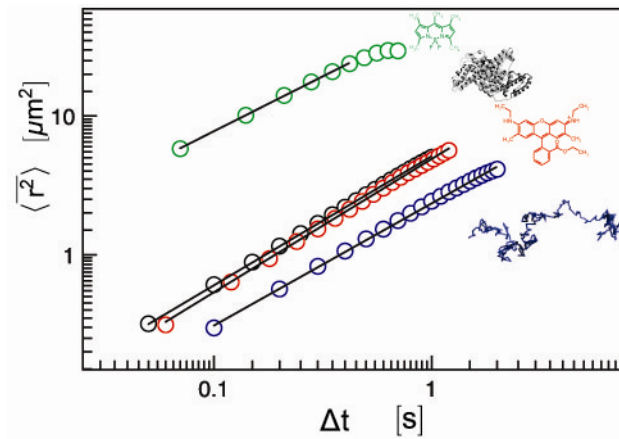


Fig. 4. (color online). Mean square displacement as a function of time.

Symbols are experimental data and solid lines are fits to the model

$$\langle r^2 \rangle = 4\Gamma(\Delta t)^\alpha. \text{ The power-law exponents are } \alpha = 0.79(2), 0.96(1), 0.93(1), \text{ and}$$

0.88(2) for BODIPY, Atto6G, BSA and PEG respectively.

Surprisingly, the mean square displacement of BSA and Atto6G scale close to linearly with time (Fig. 4), despite non-Gaussian displacement distributions. This is not unprecedented; recent work on complex fluids revealed coincidence of Fickian diffusion and non-Gaussian displacements [22]. Techniques that are sensitive only to the second



moment of the displacement distribution, such as fluorescence recovery after photobleaching (FRAP) and fluorescence correlation spectroscopy (FCS), might characterize this behavior as a single Gaussian mode of diffusion. This could explain the common interpretation of immobilization and Fickian diffusion in protein-surface studies [23]. In contrast to the linear or sub-diffusive scaling of the MSD that we observed (Fig. 4), the O'Shaughnessy model for desorption-mediated diffusion predicts super-diffusive behavior [21] given certain assumptions, including a single, characteristic desorption time  $\tau$ , which is much shorter than the time over which diffusion is observed,  $\Delta t$ . However, this assumption is not valid for our experiments, where the molecules exhibit a range of desorption times which can be on the same order as the experimental time scale, thus dampening the scaling of the MSD in the same way that intermittent trapping causes transient sub-diffusion. We also observed convergence towards a Gaussian form for some of the data (Fig. 3(b) and 3(d)), suggesting that we may be approaching the central limit in some cases. There may be some subtle deviation from the O'Shaughnessy model [21], such as imperfect sampling of the distribution or non-ideal bulk diffusion, which leads to faster recovery of the central limit and Fickian behavior.

Like in glassy systems [24], individual trajectories switched between periods of immobilization and mobility (Fig. 2(b)), so the transport cannot be described as a sum of two molecular populations. Rather, it is consistent with the so-called continuous time random walk (CTRW) model (additional evidence for intermittent dynamics is presented in the supplementary material [25]). The CTRW model was developed to describe diffusion in disordered environments and is used to describe motion that switches between immobilization and mobility [26, 27]. In contrast to a discrete random walk, in the CTRW model, the walker spends a random waiting time,  $t$ , immobilized between

each instantaneous displacement. If immobilization is due to trapping with a single binding energy  $E_b$ , the distribution of waiting times is exponential,  $\psi(t) \sim \exp(-t/\lambda)$  where  $\lambda \propto \exp(-E_b/kT)$ . When there is more than one binding energy,  $\psi(t)$  is broader than a single exponential. We measured experimental waiting times by defining a one-step distance threshold of  $0.2 \mu\text{m}$  to distinguish immobilized vibrations from true displacements (the influence of threshold on waiting times is discussed in the supplementary material [25]). For all of the molecules, the waiting times were approximately power-law distributed (suggesting a spectrum of binding energies) with a universal exponent of  $\sim 2.5$  (Fig. 5).

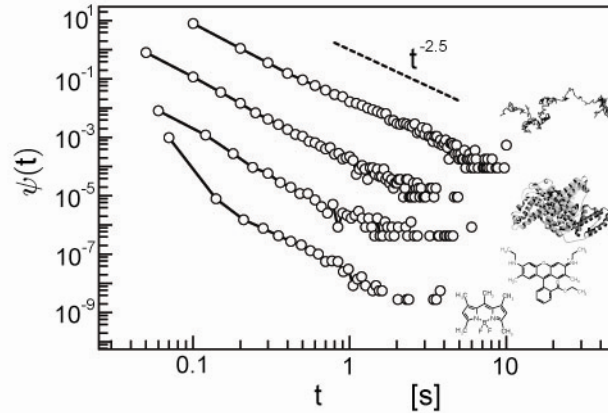


Fig. 5. Distributions of the waiting-time between surface displacements greater than  $0.2 \mu\text{m}$ . The data sets were translated vertically to allow easier interpretation (the PEG, Atto6G and BODIPY data were shifted by a factor of  $10^1$ ,  $10^{-2}$ , and  $10^{-3}$  respectively). The dashed line illustrates  $\psi(t) \sim t^{-2.5}$  behavior.

To model the experimental data, we simulated 2-dimensional CTRW dynamics using a waiting-time distribution  $\psi(t)$  and a step-size distribution  $f(r)$ . Based on our experimental observations (Fig. 5), we used a power-law for the waiting-time distribution,

$$\psi(t) = \left( (\alpha - 1) / t_s \right) \left( t_s / t \right)^\alpha$$

with a universal power-law exponent of  $\alpha = 2.5$ . During waiting

times, we assumed the noise-dependent, apparent vibrations to be Gaussian distributed,  $f_{\text{vib}}(r) \sim \exp(-r^2/2\ell^2)$ , with  $\ell = 0.065 \mu\text{m}$  dictated by our experimental localization precision. Our experimental displacement distributions and theoretical predictions [21] also suggest a power-law step-size distribution,  $f(r) = ((\beta - 1)/r_s)(r_s/r)^\beta$ . With  $\psi(t)$  and  $f(r)$ , we simulated CTRW trajectories and compared the resulting displacement distributions with the experimental data in Fig. 3 (simulation details are in [25]). We found that a universal step-size power-law exponent,  $\beta = 2.3$ , reproduced all of the experimental displacement distributions (uncertainty in  $\beta$  is discussed in the supplementary material [25]). This is the first experimental observation of power-law distributed displacements predicted for desorption-mediated surface diffusion. The distribution of desorption-mediated step lengths is predicted to scale like  $f(r) \sim r^{-1}$  and  $f(r) \sim r^{-3}$  at small and large  $r$  respectively [28]. The value of  $\beta = 2.3$  that best described our data fell within this range and lattice Monte Carlo simulations confirmed that  $f(r) \sim r^{-2.3}$  is a good description for desorption-mediated steps over a large range of length scales (see supplementary material [25]).

We found that the scale parameters,  $t_s$  and  $r_s$ , were strongly coupled in their influence on the simulated displacement distributions, so we set  $r_s = 0.2 \mu\text{m}$  (the distance threshold for the waiting-time analysis) in all the simulations, and used the waiting-time scale parameter as the only adjustable parameter in fitting the experimental data. The inverse approach, holding  $t_s$  constant and varying  $r_s$ , did not produce good fits. The waiting-time scale parameters that best described our data were  $t_s = 80, 50, 50,$  and  $5 \text{ ms}$  for PEG, BSA, Atto6G and BODIPY respectively. The waiting times systematically decreased going from the polymer to the small hydrophobic probe, consistent with smaller energy

barriers for the smaller molecules. Although the BODIPY data (Fig. 3d) could be modeled by a combination of two Gaussians, as could the BSA data at long times (Fig. 3d, blue circles), such a model could not describe the data in general. We believe that these data represent a special case of the universal model proposed where the step size distribution is approaching the central limit for reasons described above. The simulations imply that the experimental data are consistent with: 1) a broad distribution of waiting times (with a universal form) implying a spectrum of binding energies and 2) a power-law distribution of step-sizes consistent with desorption-mediated displacements.

To test whether intermittent hopping is specific to the amorphous surfaces we used, we also tracked the motion of Atto6G at an atomically-flat crystalline mica-water interface. The mica surface was prepared by gluing a 10 mm diameter mica disc (Electron Microscopy Sciences, USA) to the center of a fused silica wafer using index matched optical adhesive (NOA 84, Norland Products, USA), and reducing the mica thickness as much as possible using adhesive tape. Even at a crystalline mica surface, the dynamics were dominated by long periods of immobilization [25], similar to what we observed for Atto6G at a fused silica-water interface (data not shown). We also tested a less polar solvent, monitoring the motion of Atto6G on TMS in a tetrahydrofuran solution, where interactions other than the hydrophobic effect would dominate the dynamics. As before, the data contained the same qualitative features of intermittent dynamics that we observed at the TMS-water interface [25]. However, it is clear that the details depend on the surface chemistry and solvent. For example, the prevalence of apparent immobilization on mica could be due to a lower adsorption rate, causing most molecules to escape into the bulk after a single desorption event. The data on mica and in non-aqueous solvent are consistent with an intermittent hopping mechanism and suggest

that the non-Gaussian behavior described here is not an anomaly of the hydrophobic-water interface.,.

It was also recently shown that desorption-mediated diffusion occurs at the interface between water and high viscosity oil [29]. That result, using a homogeneous liquid-liquid interface, suggests that intermittent hopping is not simply the result of surface heterogeneity. Theoretically, however, the power-law nature of the step-size distribution is specific to strongly adsorbing systems over certain time and length scales [21], so systematic changes in physical parameters could move a system from the strongly adsorbing to the weakly adsorbing regime with consequent changes in dynamics. In future work, we will systematically investigate this parameter space and the resulting changes in surface transport.

Our observation of desorption-mediated displacements implies that the energy barriers to desorption are the same as those that control surface transport. This explains previous observations for many molecules at the solid-liquid interface [30] and contrasts with the uniform and relatively small barriers to surface diffusion in most solid-gas systems [1]. Our observation of intermittency suggests a disordered binding energy landscape. For polymers at a solid-liquid interface, a broad distribution of binding energies was previously found [31], and even a single PMMA monomer can bind to a surface under long-lived, non-equilibrium orientations [32]. Therefore, it seems plausible that a broad waiting time distribution could govern the dynamics of many molecules at a solid-liquid interface. Long periods of immobilization would dramatically affect relaxation processes like homogenization of surface coverage variations, similar to the way that long waiting times dominate viscosity in glasses. We found power-law distributed surface displacements, making large displacements much more probable than one

would predict for Gaussian-distributed displacements. Large displacements could significantly influence kinetically controlled surface processes like heterogeneous nucleation of surface structures or first-passage time dependent targeting and signaling [17]. Desorption-mediated displacements and CTRW statistics could provide a new framework for understanding and manipulating surface processes. For example, direct coupling between surface and bulk transport could be leveraged in microfluidic applications [11]. An appreciation of intermittent molecular transport at the solid-liquid interface could also reveal paths towards enhanced kinetics like those in biological systems [17].

### **Acknowledgments**

The authors acknowledge support from the U.S. Department of Energy Basic Energy Sciences, Chemical Sciences, Geosciences, and Biosciences Division (DE-SC0001854).

### **References**

- [1] T. Ala-Nissila, R. Ferrando, and S. Ying, *Adv. Phys.* **51**, 949 (2002).
- [2] M. Schunack, T. R. Linderoth, F. Rosei, E. Lægsgaard, I. Stensgaard, and F. Besenbacher, *Phys. Rev. Lett.* **88**, 156102 (2002).
- [3] R. Walder, N. Nelson, and D. K. Schwartz, *Phys. Rev. Lett.* **107**, 156102 (2011).
- [4] M. Kastantin, R. Walder, and D. K. Schwartz, *Langmuir* **28**, 12443 (2012).
- [5] M. Urbakh, J. Klafter, D. Gourdon, and J. Israelachvili, *Nature* **430**, 525 (2004).
- [6] O. Braun and A. Naumovets, *Surf. Sci. Rep.* **60**, 79 (2006).
- [7] T. Yokoyama, S. Yokoyama, T. Kamikado, Y. Okuno, and S. Mashiko, *Nature* **413**, 619 (2001).
- [8] D. K. Schwartz, *Ann. Rev. Phys. Chem.* **52**, 107 (2001).

- [9] J. V. Barth, G. Costantini, and K. Kern, *Nature* **437**, 671 (2005).
- [10] G. Erti and H. J. Freund, *Phys. Today* **52**, 32 (1999).
- [11] T. M. Squires, R. J. Messinger, and S. R. Manalis, *Nat. Biotechnol.* **26**, 417 (2008).
- [12] V. Chan, D. J. Graves, and S. E. McKenzie, *Biophys. J.* **69**, 2243 (1995).
- [13] R. Astumian and P. Chock, *J. Phys. Chem.* **89**, 3477 (1985).
- [14] O. Bénichou, C. Loverdo, M. Moreau, and R. Voituriez, *Rev. Mod. Phys.* **83**, 81 (2011).
- [15] S. A. Sukhishvili, Y. Chen, J. D. Muller, E. Gratton, K. S. Schweizer, and S. Granick, *Nature* **406**, 146 (2000).
- [16] S. C. Bae and S. Granick, *Annu. Rev. Phys. Chem.* **58**, 353 (2007).
- [17] C. Loverdo, O. Benichou, M. Moreau, and R. Voituriez, *Nat. Phys.* **4**, 134 (2008).
- [18] A. Honciuc, A. W. Harant, and D. K. Schwartz, *Langmuir* **24**, 6562 (2008).
- [19] M. J. Skaug and D. K. Schwartz, *Soft Matter* **8**, 12017 (2012).
- [20] J. P. Hansen and I. R. McDonald, *Theory of simple liquids* (Academic press, 2006).
- [21] O. V. Bychuk and B. O'Shaughnessy, *Phys. Rev. Lett.* **74**, 1795 (1995).
- [22] B. Wang, J. Kuo, S. C. Bae, and S. Granick, *Nat. Mater.* **11**, 481 (2012).
- [23] R. D. Tilton, in *Biopolymers at Interfaces*, edited by M. Martin (Marcel Dekker, Inc., 1998).
- [24] P. Chaudhuri, L. Berthier, and W. Kob, *Phys. Rev. Lett.* **99**, 060604 (2007).
- [25] See supplementary material at [\[link\]](#) for supplementary discussion and figures.
- [26] J. P. Bouchaud and A. Georges, *Phys. Rep.* **195**, 127 (1990).
- [27] J. Klafter and I. M. Sokolov, *First Steps in Random Walks, From Tools to Applications* (Oxford University Press Inc., 2011).
- [28] O. V. Bychuk and B. O'Shaughnessy, *J. Phys. II France* **4**, 1135 (1994).

- [29] I. Sriram, R. Walder, and D.K. Schwartz, *Soft Matter*. **8**, 6000 (2012).
- [30] K. Miyabe and G. Guiochon, *J. Chromatogr. A* **1217**, 1713 (2010).
- [31] B. O'Shaughnessy and D. Vavylonis, *J. Phys.: Condens. Matter* **17**, R63 (2005).
- [32] A. K. Chakraborty, J. S. Shaffer, and P. M. Adriani, *Macromolecules* **24**, 5226 (1991).